

PAPER

[View Article Online](#)
[View Journal](#) | [View Issue](#)Cite this: *J. Mater. Chem. A*, 2024, **12**, 3386Evaluating the synthesis of $\text{Mg}[\text{Al}(\text{hfp})_4]_2$ electrolyte for Mg rechargeable batteries: purity, electrochemical performance and costs†Tjaša Pavčnik,^{ab} Jernej Imperl,^b Mitja Kolar,^b Robert Dominko ^{abc} and Jan Bitenc ^{*ab}

Enhancing the performance of electrolytes stands as one of the key challenges for moving toward practical applications of Mg batteries. Within this work, we investigate different synthesis procedures for the state-of-the-art MgAlhfp electrolyte. The results show that the purity and electrochemical performance of MgAlhfp electrolytes depend on whether they are synthesized from organometallic or inorganic reagents. Additionally, electrolyte properties vary depending on the electrolyte preparation method, either *in situ* electrolyte formation or salt isolation. To improve electrolyte performance, we explore two approaches: additional salt isolation steps and the use of a scavenging additive. Salt precipitation results in a modest improvement in the coulombic efficiency of Mg plating/stripping, while a scavenging additive significantly reduces overpotentials and enhances coulombic efficiency, especially in electrolytes synthesized from inorganic reagents. Finally, investigated syntheses are evaluated in terms of their practical applicability through procedure complexity and costs of used chemicals. Based on this, we propose a synthesis procedure that strikes a balance between the electrochemical performance of Mg electrolyte and its costs.

Received 19th October 2023
Accepted 30th December 2023

DOI: 10.1039/d3ta06378j

rsc.li/materials-a

Introduction

With the ever-increasing demand for energy storage systems, the quest for sustainable and economically feasible alternatives to conventional lithium-ion batteries has intensified. Among various options, magnesium batteries have emerged as a promising alternative. One key advantage of Mg batteries is the abundance of Mg in the Earth's crust. Unlike lithium, which is considered a critical raw material by the EU and is only found in a few regions of the world,¹ Mg resources are abundant and evenly distributed, which makes Mg batteries a more sustainable choice in terms of resource availability, environmental impact, and geopolitical implications. Additionally, Mg metal has a low redox potential (-2.37 versus SHE) and offers a higher volumetric capacity ($3834 \text{ mA h cm}^{-3}$) compared to Li ($2063 \text{ mA h cm}^{-3}$), making it a promising anode material for post-lithium energy storage. However, the development of

electrolytes for Mg batteries remains an ongoing challenge, calling for further research to realize their potential.

The initial development of Mg electrolytes was based on Grignard reagent solutions, obtained through the reaction between Mg metal and organic halides. Despite exemplifying Mg plating, such electrolytes demonstrated poor oxidative stability and low ionic conductivity.² Improved oxidative stability and conductivity of electrolytes was achieved upon the addition of Lewis acids,³ resulting in the development of DCC (dichloro complex)^{4,5} and APC (all-phenyl complex)⁶ electrolytes, which enabled reversible Mg plating/stripping with high coulombic efficiency within the electrochemical window of up to 2.1 V and 3.3 V versus Mg/Mg^{2+} , respectively. Given the pyrophoric nature and nucleophilic characteristics of organometallic electrolytes, the development of Mg electrolytes focused on electrolytes with reduced reactivity, based on non-nucleophilic active species. Notably, electrolytes such as hexamethyldisilazide magnesium chloride,^{7,8} MACC (magnesium aluminate chloride complex),^{9,10} and $\text{Mg}(\text{TFSI})_2\text{-MgCl}_2$ ^{11,12} (TFSI-bis(trifluoromethanesulfonyl)imide) are less reactive and demonstrated improved oxidative stability, but fell short of delivering targeted coulombic efficiencies above 99%. Additionally, the presence of chloride species renders them corrosive towards common non-noble current collectors and cell casings, limiting their practical applications.¹³ The first chloride-free electrolyte, $\text{Mg}(\text{BH}_4)_2$, demonstrated moderate Mg plating/stripping efficiency, but suffered from limited oxidative

^aNational Institute of Chemistry, Hajdrihova 19, 1000, Ljubljana, Slovenia. E-mail: jan.bitenc@ki.si

^bFaculty of Chemistry and Chemical Technology, University of Ljubljana, Večna pot 113, 1000, Ljubljana, Slovenia

^cAlistore-European Research Institute, CNRS FR 3104, Hub de l'Energie, Rue Baudelocque, 80039, Amiens, France

† Electronic supplementary information (ESI) available. See DOI: <https://doi.org/10.1039/d3ta06378j>



stability due to the reductive nature of the BH_4^- anion.¹⁴ A milestone in Mg electrolyte development was the introduction of salts with weakly coordinating anions (WCA). MMC (magnesium mono carborane, $\text{Mg}(\text{CB}_{11}\text{H}_{12})_2$) emerged as a promising candidate, exhibiting low overpotentials (0.25 V), high coulombic efficiencies (80–94%), and high oxidative stability (3.8 V *versus* Mg/Mg^{2+}). However, the complex synthesis of carborane salt using expensive reagents could limit its practical application.¹⁵

The current golden standard of WCA-based electrolytes are fluorinated alkoxyborates and alkoxyaluminates. Among these, a specific Mg alkoxyborate, 1,1,1,3,3,3-hexafluoroisopropoxyborate ($\text{Mg}[\text{B}(\text{hfip})_4]_2$), served as a model compound and has been extensively studied in recent years. In Mg plating/stripping experiments, the $\text{Mg}[\text{B}(\text{hfip})_4]_2$ electrolyte demonstrates coulombic efficiencies above 90% and low overpotentials (70 mV). Moreover, it offers high ionic conductivities and is compatible with various cathode materials.¹⁶ An additional improvement in electrochemical properties has been observed by changing the boron central atom to aluminum. To the best of our knowledge, four studies have reported Mg $[\text{Al}(\text{hfip})_4]_2$ salt (referred to as MgAlhfip) in recent years, each following a different synthesis route. In 2016, Herb *et al.* reported an *in situ* approach where the MgAlhfip electrolyte was prepared by dissolving Mg and Al fluoroalkoxides, $\text{Mg}(\text{hfip})_2$ and $\text{Al}(\text{hfip})_3$, in ethereal solvents. The as-prepared electrolytes enabled reversible Mg plating/stripping with high coulombic efficiency (99.0% in 0.25 M electrolyte in monoglyme (G1)), exhibited oxidative stability of >3.5 V *versus* Mg/Mg^{2+} , and ionic conductivity of 6.50 mS cm^{-1} .¹⁷ A year later, Zhao-Karger *et al.* reported the MgAlhfip electrolyte, synthesized through a more robust procedure *via* an anion metathesis reaction between Na $[\text{Al}(\text{hfip})_4]$ (referred to as NaAlhfip) and MgBr_2 . The study primarily focused on the $\text{Mg}[\text{B}(\text{hfip})_4]_2$ electrolyte, providing only one cycle of CV measurement in the MgAlhfip electrolyte to confirm the reversible Mg plating/stripping.¹⁶ In 2019 Keyzer *et al.* reported on a series of Mg alkoxyaluminates, which were synthesized through a general procedure including the $\text{Mg}(\text{AlH}_4)_2$ reactant and different fluorinated alcohols. Since the synthesis of $\text{Mg}(\text{AlH}_4)_2$ includes MgCl_2 reactant, the resulting product salts contain chloride anions, which affect the electrolyte performance. A specific electrolyte, 0.25 M MgAlhfip in G1, was tested in linear sweep voltammetry experiments on different current collectors, whereby the electrolyte exhibited the highest oxidative stability of 3.0 V (*versus* Mg/Mg^{2+}) on Al. Reduced oxidative stability compared to a previous report¹⁷ was attributed to the presence of chloride in the electrolyte causing the corrosion of the electrode surface.¹⁸ In the most recent report by Mandai *et al.* (2021), MgAlhfip was synthesized through a one-pot synthesis using organometallic reagents and HFIP.¹⁹ Our group introduced an additional modification where the salt was isolated from the reaction mixture through precipitation from hexane. The electrolyte in diglyme (G2) demonstrated high performance with 99.4% coulombic efficiency of Mg plating/stripping and overpotentials below 50 mV, surpassing previously reported results.²⁰

In recent reports it has been shown that the selection of the synthesis procedure can significantly impact the purity of the product and, consequently, the electrochemical performance of electrolytes.²¹ Moreover, Yang *et al.* demonstrated that solvent quality alone can have a substantial influence on electrochemical performance in $\text{Mg}(\text{TFSI})_2$ -based electrolytes.²² As the reported MgAlhfip electrolytes have been investigated under different conditions: different solvents and concentrations, electrochemical protocols, and cell configurations, a performance comparison between the literature results is possible only to a very limited extent, and key parameters influencing the electrolyte performance cannot be assessed.

In the present work, we evaluate different synthesis procedures for the state-of-the-art MgAlhfip electrolyte. MgAlhfip electrolytes were synthesized following four reported procedures and characterized by IR and NMR spectroscopy, as well as ICP-OES. Through the electrochemical characterization of electrolytes in G2 solvent, we evaluate the use of inorganic *versus* organometallic reagents for salt synthesis. The purity of the electrolytes is identified as the key factor influencing the electrochemical performance. To enhance the latter, we follow two strategies: (i) additional salt isolation steps, which aim to improve the purity of the obtained salts, and (ii) the use of a scavenging additive, which aims to react with impurities in electrolytes and mitigate their adverse effect on the electrochemical performance. While electrochemical performance remains a decisive factor in laboratory experiments, the transition from lab-scale to commercial production necessitates a delicate equilibrium between performance and material cost. Thus, we evaluate the costs and complexity of synthesis procedures and highlight the pros and cons of each synthesis.

Experimental

All synthesis procedures, electrolytes preparation, and cell assembly were conducted in an argon-filled glovebox with water and oxygen levels below 0.1 ppm.

Syntheses of salts

1.0 M *n*-Bu₂Mg/heptane (Sigma-Aldrich), 2.0 M $\text{Al}(\text{CH}_3)_3$ /toluene (Sigma-Aldrich), $\text{Al}(\text{CH}_3)_3$ (Acr, 98%), 6–10 wt% $\text{Mg}(\text{OCH}_3)_2$ /methanol (Sigma-Aldrich), MgBr_2 (Sigma-Aldrich, 98%) and MgCl_2 (Alfa Aesar, ultra-dry, 99.9%) were used as received. NaAlH₄ (Sigma-Aldrich, 97%) was purified following a literature procedure.¹⁶ 1,1,1,3,3,3-Hexafluoroisopropanol (HFIP) (Fluorochem, 99%) and hexane (Carl Roth, >95%) were dried with 4 Å molecular sieves for 4 days before use. Tetrahydrofuran (THF) (Honeywell, >99.9%), 1,2-dimethoxyethane (G1) (Honeywell, HPLC grade, 99.9%), and diglyme (G2) (Acros Organics, extra pure, 99%) underwent a three-step drying procedure, including drying with 4 Å molecular sieves for 3 days, one day under reflux with Na/K alloy (1/3 wt%), and fractional distillation. The final water content of the as-dried solvents, determined by Karl Fischer titration, was below 1 ppm, which is the detection limit of the instrument at a specific sample volume of 5–10 mL.



MgAlhfp salts were synthesized following four literature procedures. The names of the salts correspond to the used Mg-based reactants as MgAlhfp_OME, MgAlhfp_Br, MgAlhfp_Cl, and MgAlhfp_Bu for syntheses from $\text{Mg}(\text{OCH}_3)_2$,¹⁷ MgBr_2 ,¹⁶ MgCl_2 ,¹⁸ and Bu_2Mg ¹⁹ reactants, respectively.

Synthesis of 0.4 M MgAlhfp_OME electrolyte.¹⁷ $\text{Mg}(\text{hfp})_2$ and $\text{Al}(\text{hfp})_3$ were synthesized from $\text{Mg}(\text{OCH}_3)_2$ and $\text{Al}(\text{CH}_3)_3$ by the addition of HFIP, following the literature report.¹⁷ MgAlhfp_OME electrolyte was obtained by mixing the appropriate amounts of $\text{Mg}(\text{hfp})_2$ and $\text{Al}(\text{hfp})_3$ in a 1 : 2 ratio in the selected solvent.

Synthesis of 0.4 M MgAlhfp_Br electrolyte.¹⁶ NaAlhfp was synthesized through a reported procedure.²³ The appropriate amounts of MgBr_2 and NaAlhfp in a 1 : 2 ratio were stirred for 24 hours at room temperature. The solution was filtered and the colorless filtrate was used as an electrolyte.

Synthesis of MgAlhfp_Cl salt.¹⁸ A mixture of 0.540 g (0.01 mol) NaAlH_4 and 0.476 g (0.005 mol) MgCl_2 , along with ten 10 mm diameter steel balls, was placed in a hardened steel vial with a Viton O-ring seal inside a glove box. The ball-to-powder weight ratio was approximately 35 : 1. The solids were milled in a SPEX-8000 mill for 1 hour, resulting in a powder mixture of $\text{Mg}(\text{AlH}_4)_2$ and NaCl. In a separate flask loaded with 100 mg of the $\text{Mg}(\text{AlH}_4)_2$ -containing solid and 7 mL of G1, 0.9 mL of HFIP (0.008 mol) was added dropwise. The reaction mixture was stirred at room temperature overnight. The resulting chloride-containing mixture was isolated by filtration through a PTFE membrane. A solvent from a clear colorless filtrate was removed under vacuum, yielding a white solid product, MgAlhfp_Cl.

Synthesis of MgAlhfp_Bu salt.^{19,20} HFIP (2.5 eq. *versus* Mg, 18.8 mmol, 2.0 mL) was dropwise added to a solution of *n*- Bu_2Mg in heptane (7.5 mmol, 7.5 mL). The solvent and remaining HFIP were removed under vacuum, resulting in the formation of a white powder, $\text{Mg}(\text{hfp})_2$. $\text{Mg}(\text{hfp})_2$ was dissolved in 30 mL of G1, and a solution of $\text{Al}(\text{CH}_3)_3$ in toluene (2.02 eq. *versus* Mg, 15.1 mmol, 7.6 mL) was added. Afterward, HFIP (3.5 eq. *versus* Al, 52.6 mmol, 5.6 mL) was added gradually over a period of 1 hour. After stirring at room temperature for 24 h, the solution was concentrated under reduced pressure and added to hexane to precipitate the MgAlhfp_Bu salt. The salt was filtered and dried under a vacuum at 50 °C for 48 hours.

Theoretical elemental composition of $[\text{Mg}(\text{G1})_3][\text{Al}(\text{hfp})_4]_2$: Mg 1.44, Al 3.20, O 13.29, C 25.66, F 54.12, H 2.27.

To study the effect of the isolation procedure on salt purity, additional steps were employed. MgAlhfp_OME salt was isolated from the initially *in situ* synthesized electrolyte using two methods: (i) solvent evaporation, where G1 solvent was evaporated under vacuum for 48 h at 50 °C to obtain the white solid product, and (ii) precipitation of the salt, where G1 solvent from the *in situ* electrolyte was evaporated under reduced pressure to obtain a concentrated solution, which was dropwise added into hexane to precipitate the salt. The salt was filtered and dried under vacuum for 48 h at 50 °C to obtain a white solid product. Procedure (ii) was employed also for the MgAlhfp_Cl.

Preparation of electrolytes

All electrolytes were investigated at a 0.4 M concentration, which was previously determined as the optimal composition at which the MgAlhfp electrolyte exhibited maximum ionic conductivity.¹⁹ MgAlhfp_OME and MgAlhfp_Br electrolytes were prepared *in situ* in G2 solvent, following the reported procedures.^{16,17} For electrolytes obtained from solid products, the calculated amount of the selected MgAlhfp salt was added to a measuring flask and diluted with G2 solvent to obtain a 0.4 M concentration. To investigate the impact of the scavenging additive, $\text{Al}(\text{CH}_3)_3$ was added to the prepared electrolytes at 5 or 50 mM concentration.

Characterization of salts and electrolytes

IR characterization was conducted under an inert atmosphere using an ATR-IR Alpha II (Bruker) equipped with a Ge crystal. All spectra were recorded at room temperature. Measurements were collected and averaged over 48 scans in the range of 3000 to 600 cm^{-1} . ^1H and ^{19}F NMR spectra were measured on a Bruker AVANCE NEO 600 MHz NMR spectrometer using DMSO-d_6 solvent. Chemical shifts are reported in ppm, referencing the residual solvent peak (in ^1H spectra) and trifluoroacetic acid (in ^{19}F spectra). For ICP-OES analysis, samples were prepared by weighing 100 mg of the selected salt or electrolyte into a 20 mL measuring flask and diluting it up to the mark with 1% HNO_3 solution. The concentrations of Mg, Al, and Na were measured with a 5100 ICP-OES SVDV (Agilent Technologies). Calibration standard solutions were prepared using the ICP multi-element standard solution IV (23 elements, 1000 mg L^{-1} , Sigma-Aldrich, Merck) diluted with a 1% HNO_3 solution. The calibration range was from 1 $\mu\text{g L}^{-1}$ (Mg and Al) or 3 $\mu\text{g L}^{-1}$ (Na) to 1000 $\mu\text{g L}^{-1}$. The limit of quantification (LOQ) was 1 $\mu\text{g L}^{-1}$ for Mg and Al, and 3 $\mu\text{g L}^{-1}$ for Na. The emission lines for element determination were Na at 589.592 nm, Mg at 279.553 nm, and Al at 396.152 nm. The water content of electrolytes was measured at 0.4 M salt concentration with samples of at least 0.3 g to access the detection limit of 30 ppm (LOD of 10 μg).

Electrochemical characterization

Electrochemical testing was performed in galvanostatic mode with a VMP3 potentiostat from Bio-Logic S. A. in 2-electrode Swagelok-type cells. Cells were assembled with three glassy fiber separators (GF/A, Whatman, 260 μm) wetted with approximately 100 μL of the selected electrolyte. Mg foil (0.1 mm, 99.95%, Changsha Rich Nonferrous Metals) was polished with P1200 sandpaper inside the glovebox before being used as an anode. Mg plating was performed at a current density of 1.0 mA cm^{-2} on the platinum (Pt) electrode for 1 h, followed by stripping until a cut-off voltage of 2.0 V. To ensure the result reproducibility, all electrochemical measurements were conducted in three parallel cells. The reported comparisons (absolute differences) among different data sets refer to the plotted data, which represent the middle values of the three parallel cells.



The electrochemical performance of the electrolytes was evaluated by comparing their coulombic efficiencies, overpotentials, and activation periods. The activation period corresponds to the initial cycles of battery operation, during which different electrochemical processes occur, such as the formation of an SEI layer and conditioning of electrode surfaces. The activation period was considered complete when stable cycling was achieved with observed variations in coulombic efficiency of less than 1% (absolute error). In cases where electrolytes demonstrated poor performance, stable cycling was not achieved, and the termination of the activation period was determined when the coulombic efficiency started decreasing.

Results and discussion

The synthesis of electrolytes is influenced by multiple factors, one of which is the type of reagents employed. In particular, the selection of inorganic *versus* organometallic reagents can significantly impact the complexity of the synthesis as well as the resulting properties of the electrolyte. Inorganic reagents often offer well-defined and straightforward synthesis routes, while organometallic reagents can provide more flexible ligand structures with tunable properties. In this work, the MgAlhfp was synthesized following four different procedures, two including inorganic and two including organometallic reagents (Fig. 1). Based on the source of Mg^{2+} ions in the final salt, we refer to the synthesized products as MgAlhfp_OMe, MgAlhfp_Br, MgAlhfp_Cl, and MgAlhfp_Bu when $\text{Mg}(\text{OCH}_3)_2$,

MgBr_2 ,¹⁶ MgCl_2 ,¹⁸ and Bu_2Mg ¹⁹ reactants were employed, respectively.

MgAlhfp_OMe and MgAlhfp_Br electrolytes were prepared *in situ* in G2 and were characterized in such form, if not stated otherwise. MgAlhfp_Cl and MgAlhfp_Bu were synthesized and characterized as solid salts. Note that in the original reports, MgAlhfp_Cl salt was synthesized in THF and MgAlhfp_Bu in G1 solvent.^{18,19} Solvent selection plays an important role since its molecules coordinate the Mg^{2+} cation and thus determine the structure of the salt.²⁰ To ensure a comparable structure of both synthesized salts, the MgAlhfp_Cl synthesis procedure was modified by replacing the THF solvent with G1.

The synthesized products were initially characterized by ATR-IR spectroscopy (Fig. S1†). To extract the spectra of MgAlhfp, the spectrum of G2 was subtracted from the spectra of the *in situ* electrolytes (Fig. S1a and b†). All MgAlhfp spectra exhibited characteristic peaks corresponding to the Alhfp[−] anion, consistent with previous findings reported in the literature:²⁰ Al–O–C vibration mode, and CF_3 symmetric and asymmetric stretching modes in the range of $1181\text{--}1186\text{ cm}^{-1}$, vibration modes of C– CF_3 groups and deformation mode of the $-\text{CF}_3$ groups at $1376\text{--}1379$ and $686\text{--}687\text{ cm}^{-1}$, and C–O stretching vibrations at $1092\text{--}1100\text{ cm}^{-1}$. While the spectrum of the MgAlhfp_Bu demonstrated well-defined peaks with a smooth baseline, the other spectra exhibited additional signals, particularly below 1000 cm^{-1} in the fingerprint region. Most of these undefined peaks have low to moderate intensity, and they indicate the presence of side products or other impurities.

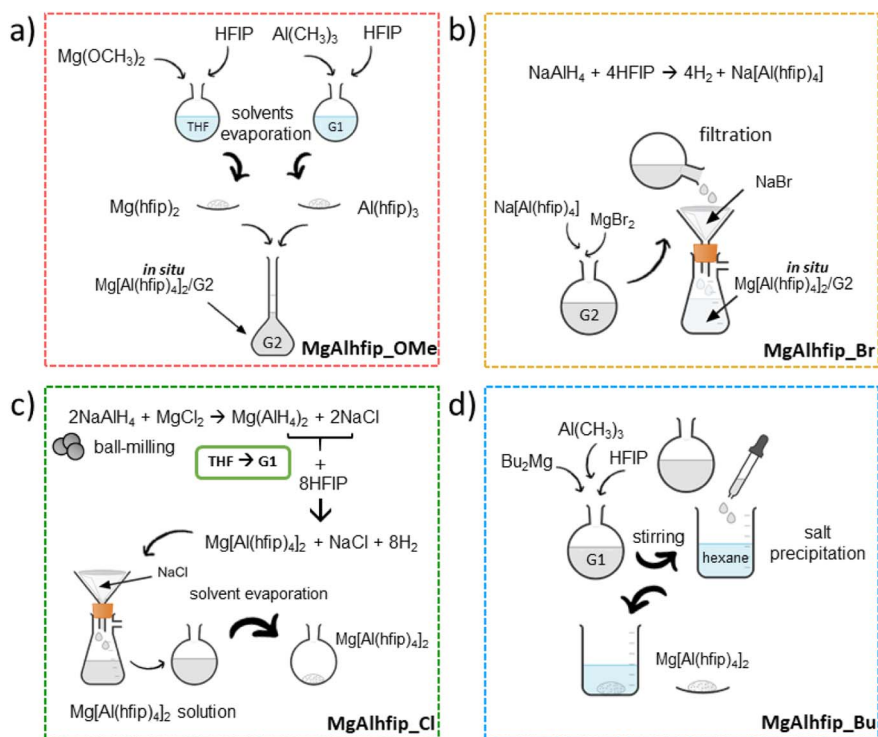


Fig. 1 Schematics of the four investigated procedures for the synthesis of MgAlhfp electrolytes. (a) MgAlhfp_OMe, (b) MgAlhfp_Br, (c) MgAlhfp_Cl, (d) MgAlhfp_Bu.



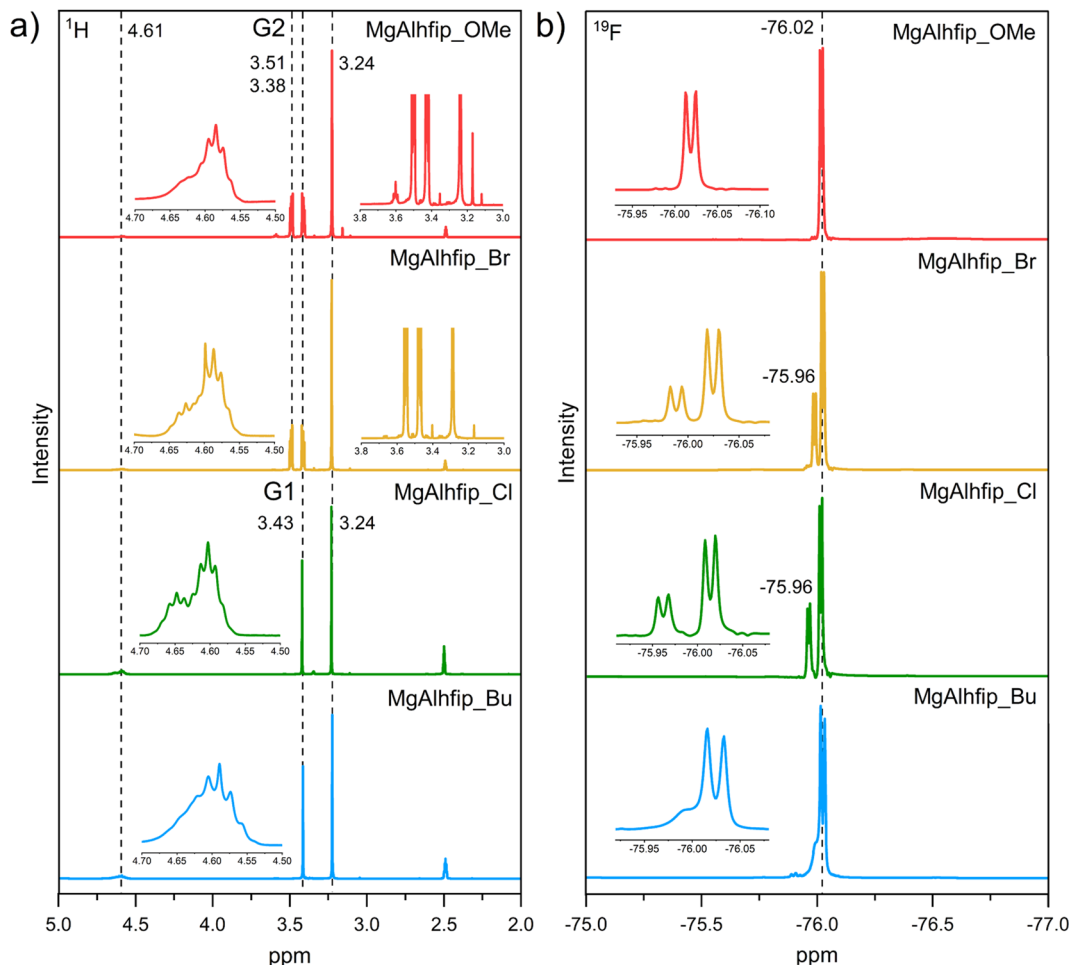


Fig. 2 (a) ^1H and (b) ^{19}F NMR spectra of MgAlhfp products synthesized by different procedures with marked characteristic peaks.

The ^1H NMR spectra of all products exhibited a prominent peak at 4.61 ppm (Fig. 2a), corresponding to the α -protons of the Alhfp $^-$ anion within the Alhfp $^-$ anion.^{19,20} In the spectra of the MgAlhfp_OMe and MgAlhfp_Br *in situ* electrolytes, additional peaks originating from the G2 solvent were observed at 3.51, 3.38, and 3.24 ppm. The MgAlhfp_Cl and MgAlhfp_Bu salts contain coordinated solvent molecules, and peaks for G1 protons were observed at 3.43 and 3.24 ppm. Additionally, both *in situ* electrolytes displayed low-intensity peaks between 3 and 4 ppm, attributed to impurities originating from the G2 solvent (Fig. S2†). Despite employing an extensive three-step drying and purification procedure on the G2 solvent, residual traces of various ethers and alcohols are still detected. This observation highlights the challenge of attaining solvents of the utmost purity, as they often come at a higher cost and may not be always available. Thus, it is necessary to strike a balance between the quality and accessibility of solvents when considering experimental protocols.

The ^{19}F NMR spectra of all MgAlhfp products displayed a prominent peak at -76.02 ppm, corresponding to the $-\text{CF}_3$ fluorine atoms of the Alhfp $^-$ anion (Fig. 2b). In the spectra of MgAlhfp_Br and MgAlhfp_Cl, an additional peak was observed at -75.96 ppm. This correlates with the ^1H spectra of

MgAlhfp_Br and MgAlhfp_Cl, where the main peak of the Alhfp $^-$ anion overlaps with an additional signal appearing at slightly higher frequencies. The overlapping peak at a comparable shift suggests the presence of a common impurity in both products. Based on the employed syntheses, the observed peak might be attributed to the NaAlhfp side product, a compound involved in both procedures. Indeed, NMR spectra of the synthesized NaAlhfp (Fig. S3†) displayed equivalent peaks and confirmed the presence of NaAlhfp in both MgAlhfp_Br and MgAlhfp_Cl products.

In the MgAlhfp_Br electrolyte, the presence of NaAlhfp may originate from an incomplete reaction between the reactants under the given conditions or a weighing error during the electrolyte preparation, resulting in a small deviation from stoichiometric amounts of both reactants. Given the small relative weighing error of 0.5%, an incomplete reaction likely makes the main contribution. Similarly, the presence of the NaAlhfp side product in the MgAlhfp_Cl salt originates from the incomplete conversion of the NaAlH_4 to $\text{Mg}(\text{AlH}_4)_2$ during the synthesis of precursors (Fig. 1c). Note that for the purpose of this work, the MgAlhfp_Cl salt was synthesized using a modified procedure where the THF solvent was replaced with G1. The synthesis in G1 solvent was preferably used since G1 molecules



coordinated to Mg^{2+} (through two oxygen atoms per one G1 molecule, bidentate binding) contribute to a more effective salt dissociation compared to THF with modest (monodentate) binding ability. Besides, $[\text{Mg}(\text{G1})_3][\text{Al}(\text{hfp})_4]_2$ salt structure is known and has been reported before,²⁰ while the structure of the salt synthesized in THF has not yet been identified.

The presence of NaAlhfp in MgAlhfp_Br and MgAlhfp_Cl products was further confirmed by ICP-OES analysis (Tables S1 and S2†), which showed deviations from the expected contents of Mg and Al and a relatively high sodium content. In the case of MgAlhfp_Br, very low bromide content excluded the significant presence of NaBr side products. Lower levels of Mg and Na and an excess of Al in the MgAlhfp_Br compared to MgAlhfp_Cl, suggest the presence of additional Al-containing compounds (such as AlR_3) in the MgAlhfp_Br product. The MgAlhfp_Cl salt contains chloride, which was reported to be present also in the THF-solvated Mg alkoxyaluminate salt and was attributed to incomplete NaCl side product elimination.¹⁸ However, the reported THF-solvated MgAlhfp product contained 3.20 wt% of Cl (determined by elemental analysis),¹⁸ while the G1-solvated MgAlhfp_Cl investigated within this work contains 35 ppm of Cl (determined by ICP-OES). Thus, by replacing the THF solvent with G1, the Cl contamination can be effectively reduced. The best agreement between the expected and measured Mg and Al contents was obtained for the MgAlhfp_OME and MgAlhfp_Bu products, which is consistent with the IR and NMR characterization indicating the lowest level of impurities in those two products. Note that small deviations in the Mg and Al content of the MgAlhfp_OME product may arise from the weighting error during electrolyte preparation. A minor deviation in Al content of MgAlhfp_Bu (+0.03) falls within the acceptable range of 2% relative standard deviation error of ICP-OES (± 0.06).

Based on the three complementary characterization methods (IR, NMR, and ICP-OES), MgAlhfp_Bu was determined as the purest product, followed by MgAlhfp_OME, which contains a low amount of impurities, although they mainly originate from the G2 solvent due to the *in situ* electrolyte preparation. MgAlhfp_Br and MgAlhfp_Cl products were identified as more contaminated, both containing NaAlhfp side product, and Al- and Cl-containing impurities additionally present.

Among different impurities, water contamination can have a substantial influence on the electrochemical performance of electrolytes. Therefore, the water content was measured in all investigated electrolytes and was 45, 95, 85, and 35 ppm for MgAlhfp_OME, MgAlhfp_Br, MgAlhfp_Cl, and MgAlhfp_Bu, respectively. We recently demonstrated that MgAlhfp has high water tolerance and reversible cycling with low overpotential was observed in the electrolytes with up to 1000 ppm of water.²⁰ The measured water content in all investigated MgAlhfp electrolytes within the present work is significantly lower (<100 ppm), thus, the electrochemical performance of organometallic and inorganic-based electrolytes is not expected to be significantly influenced by the small differences in water contamination.

The electrochemical performance of 0.4 M MgAlhfp electrolytes in G2 was evaluated through Mg plating/stripping

experiments (Fig. 3) on the Pt working electrode. The average coulombic efficiencies of Mg plating/stripping over the first 20 cycles were 97.8%, 83.0%, 96.0%, and 99.1% for MgAlhfp_OME, MgAlhfp_Br, MgAlhfp_Cl, and MgAlhfp_Bu electrolytes, respectively. Among these, MgAlhfp_Bu demonstrated the most stable performance, with only one activation cycle. In contrast, MgAlhfp_OME and MgAlhfp_Cl exhibited longer activation periods, with coulombic efficiencies gradually increasing even after 20 cycles, albeit remaining 1–3% lower compared to the MgAlhfp_Bu. MgAlhfp_Br exhibited inferior performance compared to other electrolytes, with a rapid decrease in coulombic efficiency observed after only 5 cycles (Fig. 3a). MgAlhfp_OME and MgAlhfp_Bu performed with relatively low overpotentials of 50–60 mV in cycle 10, while overpotentials in MgAlhfp_Br and MgAlhfp_Cl electrolytes were significantly higher, 400 mV and 200 mV, respectively (Fig. 3b).

MgAlhfp_OME and MgAlhfp_Bu electrolytes, both prepared through organometallic syntheses, demonstrated improved performance compared to MgAlhfp_Br and MgAlhfp_Cl electrolytes, which were synthesized from inorganic reagents (referred to as inorganic syntheses). Previous reports suggest that organometallic reagents can act as scavengers, enhancing coulombic efficiencies and reducing overpotentials.^{24,25} Although MgAlhfp_OME and MgAlhfp_Bu electrolytes were both synthesized from the organometallic reagents, MgAlhfp_Bu outperforms MgAlhfp_OME, especially in terms of coulombic efficiency. One should note that MgAlhfp_OME was prepared by dissolving Mg and Al precursors in G2 solvent, while the synthesis of the MgAlhfp_Bu was performed in G1 solvent, followed by isolation of the $[\text{Mg}(\text{G1})_3][\text{Al}(\text{hfp})_4]_2$ salt, which was then re-dissolved in G2. Therefore, the MgAlhfp_OME electrolyte contains G2 solvent exclusively, while the MgAlhfp_Bu electrolyte is a mixture of G1 from salt crystals and G2 electrolyte solvent in a 1/4 ratio (calculated for 0.4 M electrolyte concentration). It has been reported before that the G1/G2 solvent mixtures can improve the properties of electrolytes,^{12,26} which could be a reason for the differences in the electrochemical performance of MgAlhfp_OME and MgAlhfp_Bu electrolytes. To investigate this, we conducted additional experiments with the MgAlhfp_OME electrolyte in a G1/G2 = 1/4 solvent mixture. The results showed that the performance of the latter is comparable to the MgAlhfp_OME electrolyte in pure G2 solvent (Fig. S4†) and remains inferior to the MgAlhfp_Bu electrolyte with the same electrolyte composition (Fig. S5†). The G1 content in the specific solvent mixture is most likely too low to significantly affect the electrolyte properties. Consequently, the observed differences in electrochemical performance between MgAlhfp_OME and MgAlhfp_Bu electrolytes were attributed to differences in their synthesis procedures rather than minor differences in solvent composition.

A common feature of MgAlhfp_Br and MgAlhfp_Cl electrolytes that demonstrated modest performance is that they both contain NaAlhfp side product. To test the effect of the specific impurity on the electrochemical performance, NaAlhfp was added to the best-performing MgAlhfp_Bu electrolyte (Fig. S6†). In the first cycle, the coulombic efficiency of the



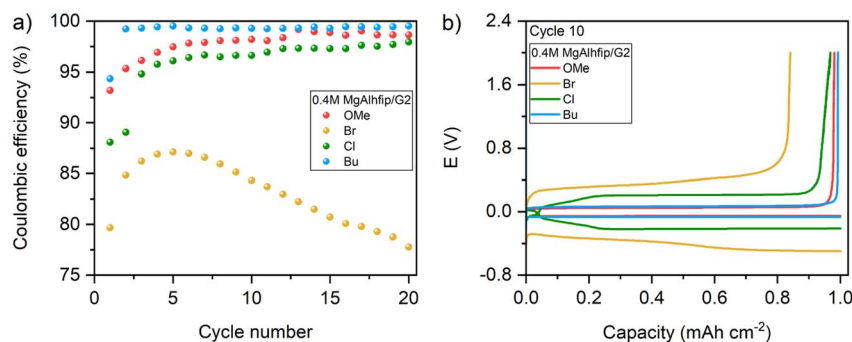


Fig. 3 Comparison of electrochemical performance of 0.4 M MgAlhfp electrolytes in G2. (a) Coulombic efficiencies of Mg plating/stripping, (b) galvanostatic curves for the 10th cycle of Mg plating/stripping. Experiments were performed at 1.0 mA cm⁻² current density.

electrolyte with the addition of NaAlhfp was similar to the pristine MgAlhfp-Bu electrolyte, however, in the following cycles, the contaminated electrolyte demonstrated inferior performance with a longer activation period, lower coulombic efficiency, and less stable cycling compared to the pristine MgAlhfp-Bu. Despite a considerable decrease in the coulombic efficiency, the Mg plating/stripping overpotential was not affected. The observed decrease in coulombic efficiency upon NaAlhfp addition can be attributed to the changes in the cation solvation structure, due to the higher concentration of Alhfp⁻ anions in the electrolyte or to the introduction of additional impurities.

It is worth noting that both MgAlhfp-Br and MgAlhfp-Cl electrolytes contain traces of halogen ions. Chloride ions are known to benefit the electrochemical performance of electrolytes with poor reductive stability, such as Mg(HDMS)₂ and Mg(TFSI)₂, electrolytes.²⁷ By contrast, our recent study showed that the addition of the MgCl₂ additive has no significant impact on the electrochemical performance of the MgAlhfp electrolyte under regular cycling conditions.²⁰ Thus, the low amount of halogen ions that are present in two MgAlhfp electrolytes prepared by inorganic-based syntheses likely does not have any beneficial effect on the electrochemical performance of investigated electrolytes.

Besides the positive effect on organometallic reagents, an improved electrolyte performance was observed when the solid salt was isolated from the reaction mixture and re-dissolved during electrolyte preparation (MgAlhfp-Bu, MgAlhfp-Cl) compared to the *in situ* electrolyte preparation (MgAlhfp-OMe, MgAlhfp-Br).

To examine the effect of the salt isolation procedure, MgAlhfp salt was first isolated from the *in situ* MgAlhfp-OMe electrolyte with two approaches (Fig. 4a): (i) solvent evaporation, where the solvent was evaporated from the MgAlhfp-OMe/G1 electrolyte by stirring the solution at the elevated temperature under vacuum. The resulting white solid was re-dissolved in G2 to obtain a 0.4 M electrolyte. For clarity, we refer to this product as *salt_{ev}*, indicating that it was obtained through solvent evaporation; and (ii) salt precipitation, where the MgAlhfp-OMe/G1 electrolyte was concentrated under reduced pressure and precipitated from hexane. The precipitated salt was filtered, additionally dried, and re-dissolved to prepare

0.4 M electrolyte in G2. We refer to this product as *salt_{prec}*, indicating that it was obtained through salt precipitation. It is important to note that both evaporation and precipitation isolation methods were employed on the *in situ* electrolyte in G1, as it is more volatile compared to G2 and can be easily evaporated.

The IR spectra of the isolated salts showed smoother baselines and well-defined peaks compared to the *in situ* electrolyte (Fig. S7†). While some minor peaks in the spectrum of the *in situ* MgAlhfp-OMe might be attributed to incomplete G2 subtraction, the presence of impurities in this electrolyte was evident. NMR characterization (Fig. 4b) additionally confirmed the enhanced purity of the isolated salts, with decreased intensity of peaks between 3 and 4 ppm. A more prominent improvement was achieved through salt precipitation, where the impurity peaks completely disappeared, resulting in a spectrum without traces of contamination.

MgAlhfp-OMe_{ev} and MgAlhfp-OMe_{prec} salts were dissolved in G2 to obtain 0.4 M electrolytes, which were tested in galvanostatic experiments (Fig. 4c). The MgAlhfp-OMe_{ev} electrolyte exhibited a slight improvement of 0.7% in coulombic efficiency during the initial three cycles compared to the *in situ* electrolyte, while the MgAlhfp-OMe_{prec} electrolyte demonstrated a 1.2–1.5% higher coulombic efficiency compared to the *in situ* electrolyte and a 0.5% higher efficiency compared to the MgAlhfp-OMe_{ev}. In the following cycles, the differences between the electrolytes diminished, and after 15 cycles, all three electrolytes performed with a coulombic efficiency of 98.5%. Although the observed variations were minor and might fall within the range of measurement errors, it is worth noting that all experiments were conducted in three parallel cells, all of which showed the same trend among three electrolytes of different purities. The purification of the MgAlhfp-OMe electrolytes did not significantly affect the cell overpotentials, and similar overpotentials of 60 mV (in cycle 10) were observed in all three electrolytes. The obtained results demonstrate a correlation between electrolyte purity and its electrochemical performance for the selected synthesis procedure. Solvent evaporation had a minimal influence on the purity of the MgAlhfp-OMe_{ev} electrolyte and, consequently, on its performance, as the isolated salt was re-dissolved in the same solvent (G2) used for the *in situ* electrolyte preparation. Salt precipitation eliminated the



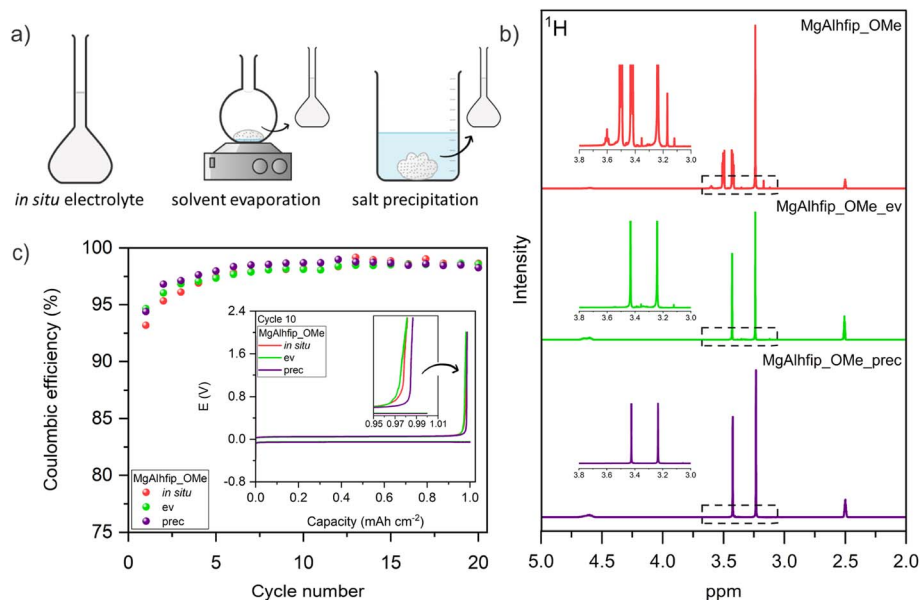


Fig. 4 (a) Schematic of three different methods for the preparation of electrolytes (from left to right): *in situ*, solvent evaporation and re-dissolution, and salt precipitation and re-dissolution, (b) ¹H NMR spectra of MgAlhfp_OMe salts of different purities, (c) coulombic efficiency of Mg plating/stripping in MgAlhfp_OMe electrolytes of different purities. Corresponding galvanostatic curves of the 10th cycle are shown as the inset.

additional, non-G2-related impurities, resulting in incremental improvement in the electrolyte's electrochemical performance during the activation period. Nonetheless, the performance of the MgAlhfp_OMe_prec is still inferior to the best-performing MgAlhfp_Bu (Fig. S8†), despite the use of similar reagents and the same salt isolation procedure in both cases. This indicates the special benefit of the MgAlhfp_Bu one-pot synthesis approach (Fig. 1d), where the reaction mixture containing organometallic reagents is stirred for a longer period of time (24 h), allowing scavenging reactions between organometallic reagents and impurities to occur.

The isolation procedure was also applied to the *in situ* MgAlhfp_Br electrolyte, however, during solvent evaporation from the 0.4 M electrolyte in G1, a gel-like compound formed. Despite extensive drying under vacuum at elevated temperatures, no solid salt could be obtained. The specific electrolyte exhibited the highest level of impurities, which most likely hindered the crystallization of the salt.²⁸ Similar difficulties were encountered when attempting salt precipitation. Thus, the impact of MgAlhfp_Br purity on its electrochemical performance could not be investigated.

Following the original procedure, MgAlhfp_Cl salt was isolated from the reaction mixture with solvent evaporation,¹⁸ thus, salt precipitation was employed as an additional isolation method, similar to the MgAlhfp_OMe_prec. In the IR spectrum of MgAlhfp_Cl_prec (Fig. S9†), low-intensity signals below 1000 cm⁻¹ are less pronounced compared to the salt obtained through solvent evaporation (MgAlhfp_Cl_ev). The ¹H NMR spectrum confirmed a reduced amount of impurities in the precipitated salt as well, although a signal for NaAlhfp was still present (Fig. S10†). This indicates that the precipitation cannot effectively separate MgAlhfp from the sodium-based side

product. ICP-OES analysis of the precipitated salt showed a slight improvement in its purity, as the measured Mg and Al contents are closer to the expected values (Table S3†). The sodium content remained high (Table S4†) due to the presence of NaAlhfp, which is consistent with the NMR results. The additional step of salt isolation did not decrease chloride-based impurities. Instead, a slight increase was observed. The overall increase of inorganic species content in the product suggests that salt precipitation primarily reduced the organic contaminants. The comparison of electrochemical performance between MgAlhfp_Cl_ev and MgAlhfp_Cl_prec electrolytes (Fig. S11†) shows similar trends as observed in MgAlhfp_OMe electrolytes of different purities. Specifically, the MgAlhfp_Cl_prec electrolyte demonstrated approximately 0.7–2.0% higher coulombic efficiency of Mg plating/stripping compared to the MgAlhfp_Cl_ev electrolyte. The improved purity did not affect the overpotentials, which remained above 200 mV in both cases.

The synthesis of MgAlhfp_Bu salt, which originally involved the precipitation step, was additionally performed by employing solvent evaporation only. The prepared electrolyte, MgAlhfp_Bu_ev, demonstrated inferior performance with 1.0% lower average coulombic efficiency compared to the original MgAlhfp_Bu electrolyte at comparable overpotentials (Fig. S12†).

Overall, all three investigated cases showed that salt precipitation can enhance the purity of the MgAlhfp salt by removing mainly organic contaminants, which results in a modest improvement of the coulombic efficiency of Mg plating/stripping in the initial cycles. However, certain side products, such as NaAlhfp as well as minor Cl-containing impurities that were present in the MgAlhfp_Cl, could not be removed by the employed procedure.



The addition of additives has proven to be an effective strategy for improving the electrochemical performance of Li-ion electrolytes.²⁹ Besides, it is a simpler and more cost-effective method than lengthy purification procedures. Thus, our second approach to enhance electrolyte performance was the addition of the scavenging (organometallic) additive. In previous reports, *n*-Bu₂Mg has typically been employed as a scavenger.^{24,25} In the present work, we selected Al(CH₃)₃ as the additive of choice, as it was used as a reagent in the synthesis of both organometallic derived electrolytes, MgAlhfp_OMe, and MgAlhfp_Bu, offering a more direct comparison as well as being commercially available in a pure form. The electrochemical characterization of MgAlhfp electrolytes, without (pristine) and with the Al(CH₃)₃ additive at 5 mM concentration is shown in Fig. 5.

The addition of the additive to the MgAlhfp_OMe electrolyte (Fig. 5a) had a beneficial impact on both the coulombic efficiency of Mg plating/stripping, as well as the duration of the activation period. In the initial cycle, the electrolyte with the additive exhibited a notably lower coulombic efficiency of Mg plating/stripping (87.3%) compared to the pristine electrolyte (93.0%). However, after the activation period, the electrolyte with the additive demonstrated a more stable performance, with 0.2–1.9% higher coulombic efficiency than the pristine electrolyte. The addition of the additive did not induce significant changes in overpotentials, which remained around 60 mV.

The MgAlhfp_Br electrolyte with 5 mM of Al(CH₃)₃ exhibited a continuous increase in coulombic efficiency, indicating a long activation period of over 20 cycles (Fig. 5b). Since MgAlhfp_Br was the most contaminated electrolyte and displayed the worst

electrochemical performance among the tested electrolytes, the additive concentration was increased to 50 mM. The increased concentration of the additive resulted in improved electrolyte performance, including a shorter activation period (11 cycles), increased coulombic efficiency (above 90% after the first cycle), a more stable performance, and overpotentials reduced to 180 mV.

Synthesis of MgAlhfp_Cl, similar to MgAlhfp_Br, did not involve any organometallic reagents. The product salt was determined to be moderately contaminated, leading to the expected noticeable effect of the scavenging additive on the electrolyte's performance. Although the effect was not as significant as in the case of MgAlhfp_Br, a clear performance improvement was observed (Fig. 5c). Electrolyte with the additive exhibited lower coulombic efficiency in the first cycle (77% *versus* 88% for the pristine electrolyte), however, in the following cycles, the electrolyte with the additive surpassed the pristine electrolyte by 2.5%. While the performance of the pristine electrolyte gradually improved during cycling, the difference after 20 cycles remained approximately 1.5% in favor of the electrolyte with the additive. Similar to the case of MgAlhfp_Br, the addition of Al(CH₃)₃ to the MgAlhfp_Cl electrolyte significantly improved the overpotentials, and values below 100 mV were observed.

In contrast, the addition of the Al(CH₃)₃ to the MgAlhfp_Bu electrolyte (Fig. 5d) resulted in marginal differences in the performance of the electrolyte with and without the additive. In both cases, the activation process lasted a single cycle, followed by stable cycling with average coulombic efficiencies of 99.5% and 99.4% for the electrolyte with and without the additive,

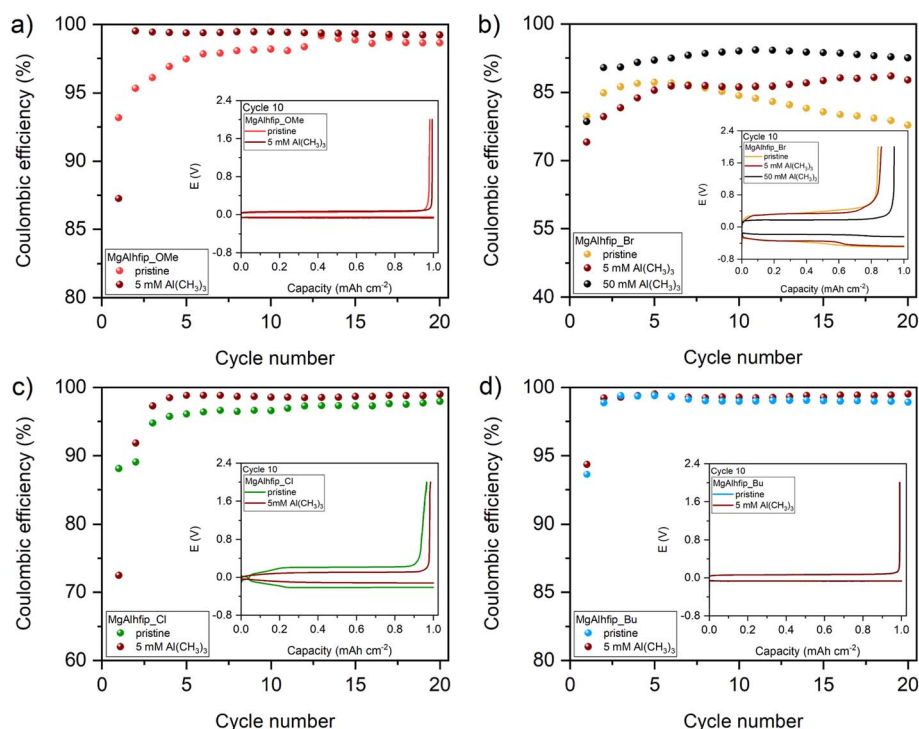


Fig. 5 Coulombic efficiency of Mg plating/stripping in (a) MgAlhfp_OMe, (b) MgAlhfp_Br, (c) MgAlhfp_Cl, and (d) MgAlhfp_Bu electrolytes with and without the Al(CH₃)₃ additive. Corresponding galvanostatic curves of the 10th cycle are shown as insets.



respectively. Overpotentials are comparable in both electrolytes, around 50 mV. As discussed above, the MgAlhfp_Bu was synthesized from organometallic reagents, which inherently scavenged impurities during the salt formation process. Thus, under the investigated conditions, the effect of the additive on the electrochemical performance of this electrolyte is minor.

Overall, the enhanced performance of MgAlhfp_OME, MgAlhfp_Br, and MgAlhfp_Cl electrolytes upon the addition of the $\text{Al}(\text{CH}_3)_3$ additive was attributed to the reduced concentration of impurities present and the potential mitigation of the passivation phenomenon on the Mg metal anode, which may occur at a slower rate. Due to the initially high purity of MgAlhfp_Bu, the influence of the additive in this electrolyte was negligible.

To probe the combined effect of both employed post-treatment procedures (salt isolation and the use of a scavenging additive), and to maximize their effect, we tested the performance of MgAlhfp_OME_ev and MgAlhfp_OME_prec (Fig. S13†), and MgAlhfp_Cl_prec (Fig. S14†) electrolytes with the addition of the $\text{Al}(\text{CH}_3)_3$ additive. The addition of the additive resulted in a further improvement in electrolyte performance, with the additive effect being the largest for less-performing electrolytes. Nevertheless, no synergistic effects could be observed when both post-treatment methods were combined.

Finally, we conducted an evaluation of the investigated syntheses, considering practical aspects such as the required time for completion, the complexity of procedures, and the costs of needed chemicals (Table 1). The syntheses of MgAlhfp_OME, MgAlhfp_Br, and MgAlhfp_Cl electrolytes are rather time-consuming, typically spanning 5–7 days, involving 3–4 steps. In contrast, the synthesis of the MgAlhfp_Bu electrolyte can be completed in two steps within a shorter timeframe of only 3 days. Details on the duration of each synthesis step are provided in Table S5.† A common feature of all investigated electrolyte syntheses is the strict safety protocol, which is required due to the use of water and air-sensitive reactants, including highly pyrophoric reactants such as $\text{Al}(\text{CH}_3)_3$, Bu_2Mg , and NaAlH_4 . To ensure controlled and safe conditions, the syntheses must be conducted in an argon or nitrogen-filled glovebox or under a Schlenk line protective atmosphere. Experienced personnel with knowledge of handling procedures are essential to minimize risks and ensure successful synthesis. Moreover, some syntheses involve additional steps that add to

their complexity (the purification of NaAlH_4 reactant for both inorganic syntheses) or require special equipment (synthesis of MgAlhfp_OME reactants at low temperature, and milling equipment for the solid-state synthesis step in the MgAlhfp_Cl synthesis procedure). From the viewpoint of synthesis complexity, MgAlhfp_Bu synthesis is a rather straightforward one-pot procedure; however, it includes the use of two organometallic reagents, which require special care during handling.

An important factor contributing to synthesis applicability is its reproducibility. Precise stoichiometry of reactants is crucial for *in situ* syntheses (MgAlhfp_OME and MgAlhfp_Br) and for the synthesis where the product is isolated through solvent evaporation only (MgAlhfp_Cl). When isolation of the product is not employed, the excess of one reactant represents impurity for the system. This issue is less pronounced when salt is precipitated (MgAlhfp_Bu), as excess reactants remain dissolved in the reaction mixture, which should result in higher reproducibility of the synthesis.

The cost of electrolytes was estimated based on the specific chemicals utilized in our experiments (Table S6†) and should be considered as a very rough small-scale comparison. The price of a given chemicals may vary depending on its purity, quantity purchased, and specific supplier. Therefore, the representation of costs for investigated syntheses serves as a general guideline only. Among the investigated procedures, the synthesis of MgAlhfp_OME is considered the most cost-effective approach, while the two inorganic synthesis protocols exhibit slightly higher costs at comparable price levels. Notably, the MgAlhfp_Bu synthesis stands out as the most expensive. A more detailed cost analysis (Fig. S15†) shows that disparities arise primarily from variations in the costs of Mg reactants and the distinct number and quantity of solvents employed in each synthesis procedure. One can note that the largest share of the costs of reactants comes from the cost of aluminum precursors. The costs of both inorganic syntheses could be significantly reduced by employing Mg reactants of lower quality. However, even when high-quality inorganic reactants were employed, such as MgCl_2 (99.9% ultra-dry) used in our synthesis, the electrolytes synthesized *via* the inorganic methods did not exhibit competitive electrochemical performance compared to electrolytes synthesized from organometallic reagents. The primary factor contributing to the high costs of the MgAlhfp_Bu synthesis is the quality and quantity of employed solvents, particularly G1, and hexane. While their consumption

Table 1 Estimation of practical aspects for different synthesis procedures of MgAlhfp electrolytes

MgAlhfp product	Synthesis time/days	Number of synthesis steps	Special requirements	Chemicals cost per mL of 0.4 M electrolyte (EUR)
MgAlhfp_OME	7	3	Work with the organometallic reagent, synthesis at low <i>T</i>	0.75
MgAlhfp_Br	5	3	Purification of NaAlH_4	1.09
MgAlhfp_Cl	5	4	Purification of NaAlH_4 , ball milling	1.04
MgAlhfp_Bu	3	2	Work with organometallic reagents	1.38



might be optimized, it cannot be entirely avoided since G1 defines the product salts by the coordination of three molecules of G1 on the Mg^{2+} cation, and hexane is used to precipitate the MgAlhfp_Bu salt from the reaction mixture, which importantly contributes to the salt's purity.

Although the MgAlhfp_Bu synthesis is costly, the specific electrolyte demonstrated the best electrochemical performance among the investigated electrolytes. In contrast, the synthesis of MgAlhfp_OMe is the most cost-effective option, but the electrolyte exhibited slightly inferior performance compared to MgAlhfp_Bu . When a scavenging additive is introduced to MgAlhfp_OMe , the performance of both electrolytes becomes more comparable (Fig. S16†) in terms of both, coulombic efficiency of Mg plating/stripping and overpotentials. Thus, we propose the use of MgAlhfp_OMe with the additive as a cost-effective alternative to MgAlhfp_Bu , offering similar electrochemical performance at significantly lower costs.

Conclusions

In the present work, we conducted a systematic evaluation of various synthesis procedures of the state-of-the-art MgAlhfp electrolyte for Mg rechargeable batteries. The obtained results highlight the critical role of the synthesis procedure in determining the purity of synthesized salts, directly influencing Mg electrolyte electrochemical performance. Specifically, electrolytes synthesized from organometallic reagents (MgAlhfp_OMe and MgAlhfp_Bu) demonstrated higher purity and better electrochemical performance compared to electrolytes prepared from inorganic reagents (MgAlhfp_Br and MgAlhfp_Cl). To enhance the performance of electrolytes, we investigated two approaches: the additional steps in salt isolation and the addition of the scavenging (organometallic) additive. Electrolytes obtained through salt precipitation displayed higher purity, leading to a slight improvement in coulombic efficiency, yet without decreasing Mg plating/stripping overpotentials. A more pronounced improvement in the electrochemical performance was observed upon the addition of the scavenging additive. Electrolytes with the $\text{Al}(\text{CH}_3)_3$ additive exhibited shorter activation periods, higher coulombic efficiencies, and decreased overpotentials. Notably, the improvement was more pronounced in more contaminated electrolytes synthesized from inorganic reagents. On the other hand, electrolytes prepared from organometallic reagents showed moderate to negligible performance improvement upon the addition of the additive. Based on the results, the synthesis of MgAlhfp_Bu emerges as the optimal procedure, combining both key steps, salt isolation and the use of organometallic reagents, resulting in the highest purity and best electrochemical performance among tested electrolytes. As a direction for future salt synthesis, we suggest the utilization of organometallic routes and precipitation of final products to minimize the amount of impurities. However, the MgAlhfp_Bu synthesis route emerged as the most expensive due to the larger consumption of solvents. Considering the cost optimization, an alternative approach involving the use of the additive in a more cost-effective synthesis procedure might present a viable solution

to strike a balance between electrolyte effectiveness and costs. Nevertheless, it is important to note that targeted Mg metal plating/stripping efficiencies above 99.9% are yet to be achieved and will be together with material cost a key performance indicator for practical rechargeable Mg metal batteries.

The insights gained in this study provide guidelines for future Mg electrolyte synthesis, which can speed up the development of next-generation Mg electrolytes with improved electrochemical performance.

Conflicts of interest

There are no conflicts to declare.

Acknowledgements

T. P., R. D., and J. B. would like to acknowledge the financial support of the Slovenian Research Agency through research program P2-0423 and research projects N2-0279 and J2-4462, while J. I. and M. K. acknowledge funding from the same agency through research program P1-0153.

References

- European Commission, Directorate-General for Internal Market Industry, S. Bobba, S. Carrara, J. Huisman, F. Mathieux and C. Pavel, Critical Raw Materials for Strategic Technologies and Sectors in the EU -, *A Foresight Study*, 2020.
- L. W. Gaddum and H. E. French, *J. Am. Chem. Soc.*, 1927, **49**, 1295–1299.
- T. Liu, Y. Shao, G. Li, M. Gu, J. Hu, S. Xu, Z. Nie, X. Chen, C. Wang and J. Liu, *J. Mater. Chem. A*, 2014, **2**, 3430–3438.
- D. Aurbach, H. Gizbar, A. Schechter, O. Chusid, H. E. Gottlieb, Y. Gofer and I. Goldberg, *J. Electrochem. Soc.*, 2002, **149**, A115.
- D. Aurbach, Z. Lu, A. Schechter, Y. Gofer, H. Gizbar, R. Turgeman, Y. Cohen, M. Moshkovich and E. Levi, *Nature*, 2000, **407**, 724–727.
- N. Pour, Y. Gofer, D. T. Major and D. Aurbach, *J. Am. Chem. Soc.*, 2011, **133**, 6270–6278.
- C. Liebenow, Z. Yang and P. Lobitz, *Electrochem. Commun.*, 2000, **2**, 641–645.
- C. Liao, N. Sa, B. Key, A. K. Burrell, L. Cheng, L. A. Curtiss, J. T. Vaughey, J. J. Woo, L. Hu, B. Pan and Z. Zhang, *J. Mater. Chem. A*, 2015, **3**, 6082–6087.
- R. E. Doe, R. Han, J. Hwang, A. J. Gmitter, I. Shterenberg, H. D. Yoo, N. Pour and D. Aurbach, *Chem. Commun.*, 2014, **50**, 243–245.
- J. H. Ha, B. Adams, J. H. Cho, V. Duffort, J. H. Kim, K. Y. Chung, B. W. Cho, L. F. Nazar and S. H. Oh, *J. Mater. Chem. A*, 2016, **4**, 7160–7164.
- Y. Cheng, R. M. Stolley, K. S. Han, Y. Shao, B. W. Arey, N. M. Washon, K. T. Mueller, M. L. Helm, V. L. Sprenkle, J. Liu and G. Li, *Phys. Chem. Chem. Phys.*, 2015, **17**, 13307–13314.



- 12 S. Y. Ha, Y. W. Lee, S. W. Woo, B. Koo, J. S. Kim, J. Cho, K. T. Lee and N. S. Choi, *ACS Appl. Mater. Interfaces*, 2014, **6**, 4063–4073.
- 13 J. Muldoon, C. B. Bucur, A. G. Oliver, J. Zajicek, G. D. Allred and W. C. Boggess, *Energy Environ. Sci.*, 2013, **6**, 482–487.
- 14 R. Mohtadi, M. Matsui, T. S. Arthur and S. J. Hwang, *Angew. Chem., Int. Ed.*, 2012, **51**, 9780–9783.
- 15 O. Tutusaus, R. Mohtadi, T. S. Arthur, F. Mizuno, E. G. Nelson and Y. V. Sevryugina, *Angew. Chem., Int. Ed.*, 2015, **54**, 7900–7904.
- 16 Z. Zhao-Karger, M. E. Gil Bardaji, O. Fuhr and M. Fichtner, *J. Mater. Chem. A*, 2017, **5**, 10815–10820.
- 17 J. T. Herb, C. A. Nist-Lund and C. B. Arnold, *ACS Energy Lett.*, 2016, **1**, 1227–1232.
- 18 E. N. Keyzer, J. Lee, Z. Liu, A. D. Bond, D. S. Wright and C. P. Grey, *J. Mater. Chem. A*, 2019, **7**, 2677–2685.
- 19 T. Mandai, Y. Youn and Y. Tateyama, *Mater. Adv.*, 2021, **2**, 6283–6296.
- 20 T. Pavčnik, M. Lozinšek, K. Pirnat, A. Vizintin, T. Mandai, D. Aurbach, R. Dominko and J. Bitenc, *ACS Appl. Mater. Interfaces*, 2022, **14**, 26766–26774.
- 21 T. Mandai, *ACS Appl. Mater. Interfaces*, 2020, **12**, 39135–39144.
- 22 Z. Yang, M. Yang, N. T. Hahn, J. Connell, I. Bloom, C. Liao, B. J. Ingram and L. Trahey, *Front. Chem.*, 2022, **10**, 937.
- 23 S. Murugan, S. Niesen, J. Kappler, K. Küster, U. Starke and M. R. Buchmeiser, *Batteries Supercaps*, 2021, **4**, 1636–1646.
- 24 I. Shterenberg, M. Salama, H. D. Yoo, Y. Gofer, J.-B. Park, Y.-K. Sun and D. Aurbach, *J. Electrochem. Soc.*, 2015, **162**, A7118–A7128.
- 25 T. Pavčnik, J. Bitenc, K. Pirnat and R. Dominko, *Batteries Supercaps*, 2021, **4**, 815–822.
- 26 H. Dong, O. Tutusaus, Y. Liang, Y. Zhang, Z. Lebens-Higgins, W. Yang, R. Mohtadi and Y. Yao, *Nat. Energy*, 2020, **5**, 1043–1050.
- 27 S. He, K. V. Nielson, J. Luo and T. L. Liu, *Energy Storage Mater.*, 2017, **8**, 184–188.
- 28 S. Dobberschütz, M. R. Nielsen, K. K. Sand, R. Civioc, N. Bovet, S. L. S. Stipp and M. P. Andersson, *Nat. Commun.*, 2018, **9**, 1578.
- 29 K. Xu, *Chem. Rev.*, 2014, **114**, 11503–11618.

